

# Optical study of the metal-insulator transition in $\text{CuIr}_2\text{S}_4$ crystals

N. L. Wang,<sup>1,\*</sup> G. H. Cao,<sup>2</sup> P. Zheng,<sup>1</sup> G. Li,<sup>1</sup> Z. Fang,<sup>1</sup> T. Xiang,<sup>3</sup> H. Kitazawa,<sup>4</sup> and T. Matsumoto<sup>4</sup>

<sup>1</sup>*Institute of Physics and Center for Condensed Matter Physics,  
Chinese Academy of Sciences, P. O. Box 603, Beijing 100080, P. R. China*

<sup>2</sup>*Department of Physics, Zhejiang University, Hangzhou 310027, P. R. China*

<sup>3</sup>*Institute of Theoretical Physics and Interdisciplinary Center of Theoretical Studies,  
Chinese Academy of Sciences, Beijing 100080, P. R. China*

<sup>4</sup>*National Institute for Materials Science, Sengen 1-2-1, Tsukuba, Ibaraki 305-0047, Japan*

We present measurements of the optical spectra on single crystals of spinel-type compound  $\text{CuIr}_2\text{S}_4$ . This material undergoes a sharp metal-insulator transition at 230 K. Upon entering the insulating state, the optical conductivity shows an abrupt spectral weight transfer and an optical excitation gap opens. In the metallic phase, Drude components in low frequencies and an interband transition peak at  $\sim 2\text{eV}$  are observed. In the insulating phase, a new peak emerges around  $0.5\text{eV}$ . This peak is attributed to the transition of electrons from the occupied  $\text{Ir}^{3+} t_{2g}$  state to upper  $\text{Ir}^{4+} t_{2g}$  subband resulting from the dimerization of  $\text{Ir}^{4+}$  ions in association with the simultaneous formations of  $\text{Ir}^{3+}$  and  $\text{Ir}^{4+}$  octamers as recently revealed by the x-ray diffraction experiment. Our experiments indicate that the band structure is reconstructed in the insulating phase due to the sudden structural transition.

PACS numbers: 72.80.Ga, 78.20.Ci, 71.30.+h, 78.30.-j

Spinel type compound  $\text{CuIr}_2\text{S}_4$  has recently attracted much attention for its intriguing first-order metal-insulator transition (MIT) at  $T_{MI} \sim 230 \text{ K}$ <sup>1,2,3,4,5,6,7,8,9,10,11,12,13,14,15</sup>. The transition is characterized by a sudden increase of the electrical resistivity, a disappearance of Pauli paramagnetism, a hysteresis loop in resistivity  $\rho$  and magnetic susceptibility  $\chi$ , and a lowering of structure symmetry. Above the MIT temperature,  $\text{CuIr}_2\text{S}_4$  has a normal cubic spinel structure, in which the Cu ions (A sites) are tetrahedrally coordinated and the Ir ions (B sites) are octahedrally coordinated by sulfur ions. Upon entering the low temperature insulating phase, a structural deformation occurs, lowering the lattice symmetry to triclinic<sup>11</sup>.

The structure and the MIT in  $\text{CuIr}_2\text{S}_4$  is reminiscent of a classic spinel compound—the magnetite  $\text{Fe}_3\text{O}_4$ , which also exhibits an abrupt MIT at about 120 K, called the Verway transition<sup>16</sup>. The  $\text{Fe}_3\text{O}_4$  undergoes a ferrimagnetic transition at a much higher temperature (858 K). Below this temperature, the magnetic moments of the Fe ions are ferrimagnetically ordered, but the A sites [ $\text{Fe}^{3+} (t_{2g}^3 e_g^2, s=5/2)$ ] and B sites [ $\text{Fe}^{2+} (t_{2g}^4 e_g^2, s=2)$  and  $\text{Fe}^{3+} (s=5/2)$ ] have opposite spin directions. The Verway transition has been interpreted as a charge ordering transition of  $\text{Fe}^{2+}$  and  $\text{Fe}^{3+}$  on the B sites in alternate (001) planes<sup>17</sup>.

Naturally, it is considered that the MIT in  $\text{CuIr}_2\text{S}_4$  is similar to the Verway transition in  $\text{Fe}_3\text{O}_4$ . Since the band structure calculation and the photoemission experiments revealed that the valence state of Cu is  $\text{Cu}^{1+3,4}$ , it is believed that the ionic configuration of  $\text{Cu}^{1+}\text{Ir}^{3+}\text{Ir}^{4+}\text{S}_4^{2-}$  is realized in the low-T insulating phase, and the ordering of  $\text{Ir}^{3+}$  and  $\text{Ir}^{4+}$  ions is a plausible origin of the MIT<sup>4,10</sup>. Indeed, recent high-resolution synchrotron X-ray powder diffraction experiment revealed a peculiar form of charge ordering which consists of alternating arrangement of iso-

morphic octamers or clusters of  $\text{Ir}_8^{3+}\text{S}_{24}$  and  $\text{Ir}_8^{4+}\text{S}_{24}$  (as isovalent bi-capped hexagonal rings) together with spin-dimerizations between  $\text{Ir}^{4+}$  ions<sup>11</sup>. The charge-ordering pattern is much more complicated than  $\text{Fe}_3\text{O}_4$  as well as any other previously known charge-ordered structures which are typically based on stripes, slabs or checkerboard patterns. The simultaneous charge-ordering and spin-dimerization transition is a rare phenomenon in three-dimensional compounds<sup>11</sup>. Therefore, it is very interesting to further explore how the electronic structures change in the MIT. This work presents a detailed infrared spectroscopy study on single crystal samples. It provides important information about low-lying excitations across the transition.

Single crystals of  $\text{CuIr}_2\text{S}_4$  were grown from the bismuth solution<sup>18</sup>. First, single phase  $\text{CuIr}_2\text{S}_4$  powders were synthesized by solid-state reaction in sealed quartz tube using high purity (better than 4N) powders of elements Cu, Ir, and S as starting materials. Then,  $\text{CuIr}_2\text{S}_4$  and metal bismuth (6N) in the molar ratio of 1:100 were sealed in an evacuated quartz ampoule. The ampoule was heated to 1273 K, and holding for two days. Crystals of  $\text{CuIr}_2\text{S}_4$  were grown by cooling at 4 K/hour down to 773 K. Typically, the crystals have triangular shape of surface with edge length about 0.4 mm. The near-normal incidence reflectance spectra were measured by using a Bruker 66v/S spectrometer in the frequency range from  $100 \text{ cm}^{-1}$  to  $28000 \text{ cm}^{-1}$ . The sample was mounted on an optically black cone in a cold-finger flow cryostat. An *in situ* overcoating technique was employed for reflectance measurement<sup>19</sup>, which enables us to get reliable data on small-size samples. The spectra above  $500 \text{ cm}^{-1}$  was collected on one single crystal, while the data in the far-infrared regime was obtained on mosaic crystal samples. The optical conductivity spectra were obtained from a Kramers-Kronig transformation of  $R(\omega)$ .

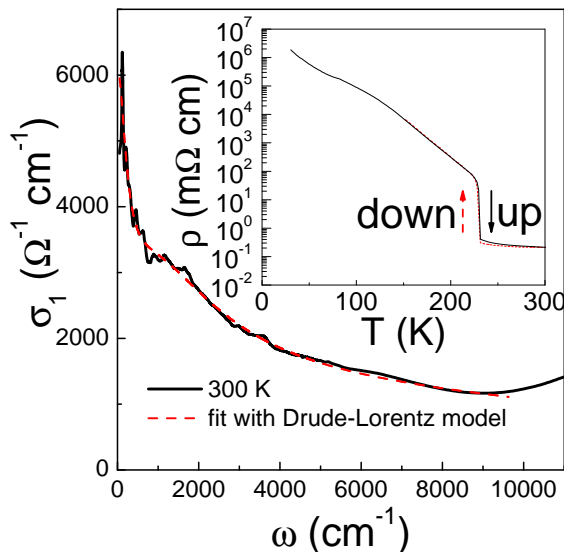


FIG. 1: (Color online) The optical conductivity spectrum of  $\text{CuIr}_2\text{S}_4$  at 300 K. Dashed curve is a fit to the data using two Drudes and one Lorentz components. The inset shows T-dependence of dc resistivity as the sample was cooled down and warmed up.

We use Hagen-Rubens' relation for the low frequency extrapolation, and a constant extrapolation to  $80000 \text{ cm}^{-1}$  followed by a well-known function of  $\omega^{-4}$  in the higher-energy side.

Fig. 1 shows the room-T optical conductivity below  $11000 \text{ cm}^{-1}$ . The dc resistivity as a function of temperature is shown in the inset. There is a sharp metal-insulator transition at 230 K. The optical spectrum shows an usual metallic response with a conductivity minimum around  $9000 \text{ cm}^{-1}$ . The spectrum could be well fitted with two Drude components and a Lorentz oscillator below the frequency of minimum conductivity. The two Drude components, which result from bands crossing the Fermi energy, have plasma frequencies and scattering rates of  $\omega_{p1} \approx 7000 \text{ cm}^{-1}$ ,  $\Gamma_1 \approx 250 \text{ cm}^{-1}$  and  $\omega_{p2} \approx 20000 \text{ cm}^{-1}$ ,  $\Gamma_2 \approx 2400 \text{ cm}^{-1}$ , respectively. The Lorentz part has a central frequency of  $4000 \text{ cm}^{-1}$  ( $0.5 \text{ eV}$ ).

Fig. 2 shows the reflectance and optical conductivity spectra at different temperatures over broad frequencies. The spectra show little change as temperature decreases from 300 K to 232 K, except in the very low-frequency region. However, upon entering the insulating phase, dramatic change occurs in optical spectra. The low- $\omega$  spectral weight below  $0.5 \text{ eV}$  ( $4000 \text{ cm}^{-1}$ ) is severely suppressed, resulting in the opening of an optical gap. The missing spectral weight is transferred to higher energies, forming a pronounced peak ( $\alpha$ ) at  $0.5 \text{ eV}$ . In addition, another peak (labelled as  $\beta$ ) exists around  $2 \text{ eV}$  ( $16000 \text{ cm}^{-1}$ ). This peak is also present in the metallic state in high temperatures at slightly higher frequency. The strong suppression of the low-energy spectral weight and the two-peaks ( $\alpha$  and  $\beta$ ) structure are the most pronounced features below  $T_{MI}$ .

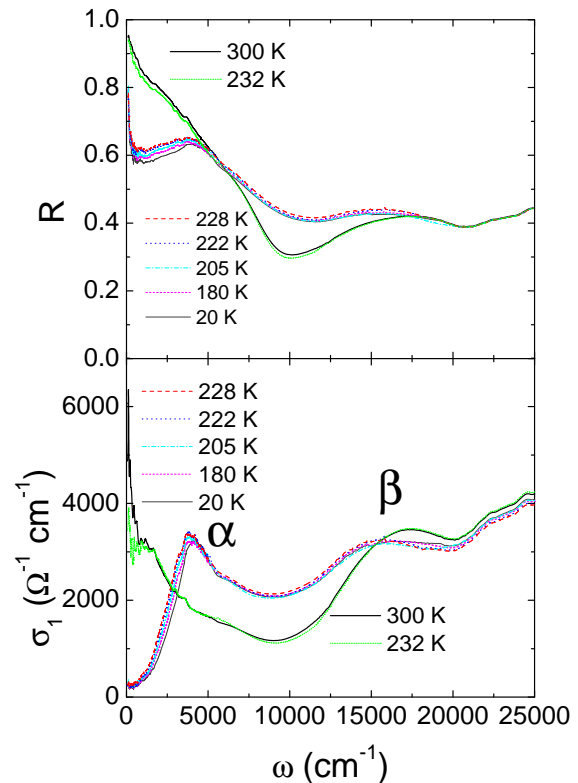


FIG. 2: (Color online) Temperature dependence of the reflectivity spectra (up panel) and optical conductivity spectra (bottom panel) for a  $\text{CuIr}_2\text{S}_4$  single crystal with  $T_{MI}=230 \text{ K}$ . Abrupt spectral change occurs at  $T_{MI}$ .

Understanding the above spectral change, which is the main task of this work, is crucial for the understanding of the change of electronic structures above and below  $T_{MI}$ . Because Cu at A site is in the  $\text{Cu}^{1+}$  valence state ( $3d^{10}$ )<sup>4</sup>, the Cu 3d band is fully filled. The band structure calculations indicate that the Cu 3d band locates at about  $3 \text{ eV}$  below  $E_F$ .<sup>3</sup> Thus the MIT and the accompanied change is mainly due to the variation of the electronic states of 5d transitional metal Ir. Due to the crystal field and the hybridization between Ir 5d and S 3p orbitals, the splitting of the  $e_g$  and  $t_{2g}$  bands of Ir 5d electrons is fairly large.<sup>20</sup> As a result, a low-spin state of Ir 5d electrons is favored. The Ir  $e_g$  band is empty and the states near Fermi level are mainly contributed by the Ir  $t_{2g}$  bands, but hybridized with S 3p orbitals.

Let us begin our discussion with the metallic phase in which  $\text{CuIr}_2\text{S}_4$  has normal cubic spinel structure. There is only one equivalent position for Ir in the structure with a valence state of  $\text{Ir}^{+3.5}$  and the Ir 5d band is partially filled. Band structure calculation indicates that two bands arising from the hybridization of Ir  $5d\epsilon$  (i.e.  $t_{2g}$ ) and S 3p cross the Fermi energy<sup>3</sup>. These two bands lead to the Drude responses in low frequencies. In this case, the electronic state could be understood from the schematic picture of Fig. 3(a).

Upon entering the insulating state, a first-order struc-

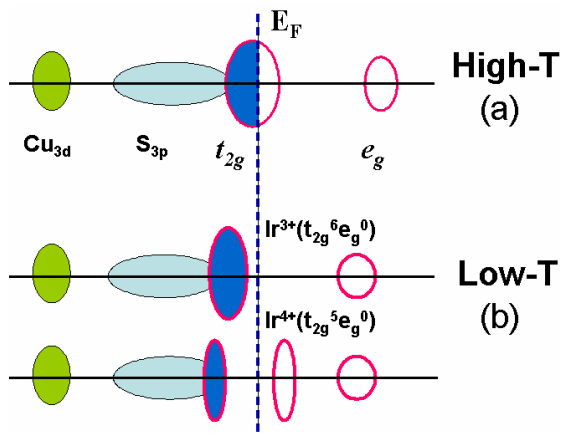


FIG. 3: (Color online) Schematic diagrams of the electronic states above and below the MIT temperature. The enclosed areas above and below the horizontal lines represent the spin-up and spin-down states. (a) Above  $T_{MI}$ ,  $\text{Ir}^{3.5}$  has partially filled  $t_{2g}$  bands. (b) Below  $T_{MI}$ , the structure contains only  $\text{Ir}^{3+}$  and  $\text{Ir}^{4+}$  octamers.  $\text{Ir}^{3+}$  has fully filled  $t_{2g}$  band and completely empty  $e_g$  band. The  $\text{Ir}^{4+}$  should have a partially filled band in one of  $t_{2g}$  orbitals. However, the dimerization of  $\text{Ir}^{4+}$  makes the band split into two subbands.

tural phase transition occurs and the lattice symmetry becomes triclinic<sup>11</sup>. Most remarkably,  $\text{CuIr}_2\text{S}_4$  undergoes a complex charge-ordering transition. A group of 8  $\text{Ir}^{3+}$  or  $\text{Ir}^{4+}$  octahedra forms a cluster called octamer, which can be viewed as planar hexagonal rings with two additional octahedra attached to the opposite sides. The Ir ions in the  $\text{Ir}^{4+}$  octamers exhibits drastic alternations of long and short Ir-Ir distances, whereas the Ir-Ir distance in  $\text{Ir}^{3+}$ -octamers are uniform<sup>11</sup>. These structural features reveal important clues for the understanding of the low-T optical spectra. Because of the low-spin state of Ir ions,  $\text{Ir}^{3+}$  has fully filled  $t_{2g}$  bands and completely empty  $e_g$  band. Therefore, the  $\text{Ir}^{3+}$  (spin  $s=0$ ) octamers are insulating. The  $\text{Ir}^{4+}$  has  $t_{2g}^5 e_g^0$  configuration (spin  $S=1/2$ ) and one of the  $t_{2g}$  orbitals is half filled. In principle, a material with a half filled band should be metallic. However, the dimerization of  $\text{Ir}^{4+}$  ions splits this band into two subbands. The lower subband is fully occupied while the upper subband is empty (Fig. 3b). Since the  $\alpha$  peak appears only in the insulating phase, it is reasonable to attribute the  $\alpha$  peak to the transition of electrons from the occupied  $\text{Ir}^{3+} t_{2g}$  or lower  $\text{Ir}^{4+} t_{2g}$  to upper  $\text{Ir}^{4+} t_{2g}$  subband. Since the transition of electrons from  $\text{Ir}^{4+}$  site to  $\text{Ir}^{4+}$  site actually requires to overcome additional on-site Coulomb repulsion energy, it is plausible that the lowest excitation is from  $\text{Ir}^{3+} t_{2g}$  state to upper  $\text{Ir}^{4+} t_{2g}$  subband. This is equivalent to say that the  $\alpha$  peak is originated from the inter-octamer hoppings. The  $\beta$  peak comes from the transition of electrons from the occupied Ir  $t_{2g}$  to the empty Ir  $e_g$  bands. Since the unoccupied Ir  $e_g$  bands exist at temperature higher than the MIT, the  $\beta$  component is observable even in the metallic phase. This is the reason why the temperature-dependence of the  $\beta$

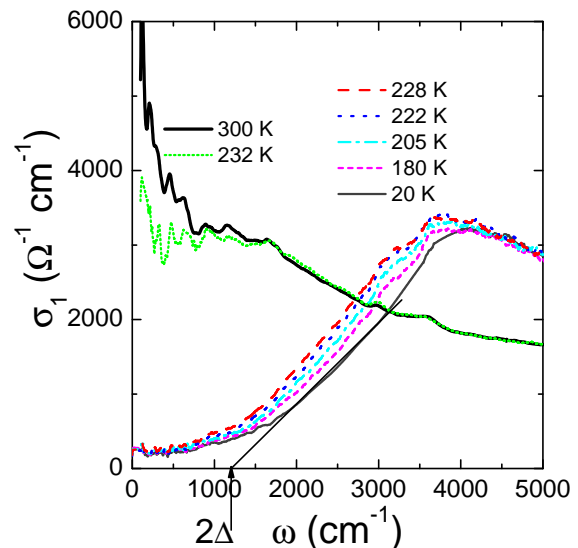


FIG. 4: (Color online) The temperature dependence of the optical conductivity in an expanded scale at low frequencies. A thin straight line is extrapolation of the onset of the peak for the estimate of the magnitude of the optical gap.

peak is different from that of the  $\alpha$  one. The interband transition from Cu 3d to other unoccupied state should appear at higher energies.

The optical data and the analysis provide a clear picture about the change of electronic structures above and below the MIT temperature. The high-T metallic state is due to the band conduction of hybridized Ir  $t_{2g}$  and S 3p electrons. In the insulating state, the formation of the  $\text{Ir}^{3+}$  and  $\text{Ir}^{4+}$  octamers results in two different types of insulating clusters.  $\text{Ir}^{3+}$  octamers have fully occupied Ir  $t_{2g}$  bands, whereas  $\text{Ir}^{4+}$  octamers produce two splitting subbands because of the  $\text{Ir}^{4+}$ - $\text{Ir}^{4+}$  dimerization. Furthermore, the dimerized  $\text{Ir}^{4+}$  ions form a spin singlet. It suppresses the Pauli paramagnetism of  $\text{CuIr}_2\text{S}_4$  and leads to the diamagnetic nature of the insulating state<sup>10</sup>.

The above discussion on the evolution of the electronic states is consistent with a recent S  $K$  and Ir  $L_3$  x-ray absorption study on  $\text{CuIr}_2\text{S}_4$  by Croft et al.<sup>15</sup> where similar redistribution of Ir 5d electronic states across the MIT has been proposed. Apparently, the MIT of  $\text{CuIr}_2\text{S}_4$  is different to the Verway transition in  $\text{Fe}_3\text{O}_4$ .  $\text{Fe}_3\text{O}_4$  contains relatively narrow 3d band and the charge ordering is most likely caused by the competition between the bandwidth and strong intersite Coulomb repulsion<sup>17,21</sup>. However,  $\text{CuIr}_2\text{S}_4$  is expected to have a wide 5d band and weaker Coulomb repulsion. The MIT in  $\text{CuIr}_2\text{S}_4$  is due to the reconstruction of Ir 5d bands associated with the structural change.

Our result shows unambiguously that the MIT in  $\text{CuIr}_2\text{S}_4$  is directly correlated with the structural instability. It seems that this structural instability is unique in the  $\text{CuIr}_2\text{S}_4$  family. Any substitution to A-sites (e.g. Zn for Cu)<sup>10,14</sup> or B-sites (e.g. Rh for Ir)<sup>6</sup> or S-sites (e.g. Se for S)<sup>5</sup> will suppress the structural deformation and

drive the compound into metallic or superconducting in low temperatures. The strong electron-phonon coupling is the most probable mechanism responsible for the structural instability. Further theoretical and experimental efforts to the understanding of this mechanism are desired.

Fig. 4 shows the low- $\omega$  conductivity spectra in an expanded scale. Below the MIT temperature, the optical conductivity increases quickly above  $1000\text{ cm}^{-1}$ . A rough estimation of the optical gap could be obtained by extrapolating the linear increasing part to the base line of  $\sigma(\omega)=0$ . This gives the value of the optical gap  $2\Delta \sim 1200\text{ cm}^{-1}$  ( $0.15\text{ eV}$ ). The gap magnitude ( $\Delta$ ) is close to the activated gap values estimated from several dc resistivity measurements<sup>1,2</sup>. Matsuno et al. performed photoemission measurements on  $\text{CuIr}_2\text{S}_4$ , but assigned a much smaller gap amplitude of  $\sim 20\text{ meV}$  in the insulating phase<sup>4</sup>. However, by looking at their spectral curves at 250 K and 30 K, we found that the spectral edge actually shifts about 70 to 80 meV away from the Fermi level, and seemed to be consistent with our experiment. Additionally, we found that the energy gap changes very little as the temperature increases from 10

K to 228 K. The sudden opening of the energy gap below MIT is associated with the structural transition, and is a characteristic feature of the first-order structural phase transition.

To conclude, optical conductivity spectra have been investigated for single crystals of  $\text{CuIr}_2\text{S}_4$ . The metallic response at high temperature is due to the band conduction of Ir  $t_{2g}$  electrons, which are hybridized with S  $3p$  electrons. The MIT in  $\text{CuIr}_2\text{S}_4$  is caused by the reconstruction of Ir 5d bands associated with the structural change. The formations of the  $\text{Ir}^{3+}$  and  $\text{Ir}^{4+}$  octamers below  $T_{MI}$  result in two different types of insulating clusters. We attribute the  $\alpha$  peak to the transition of electrons from the occupied  $\text{Ir}^{3+} t_{2g}$  state to upper  $\text{Ir}^{4+} t_{2g}$  subband created by the spin-dimerization in the  $\text{Ir}^{4+}$  octamers, and the  $\beta$  component to the transition from the occupied Ir  $t_{2g}$  to the empty Ir  $e_g$  bands.

This work is supported by National Science Foundation of China (No. 10025418, 10104012, 10374109), the Knowledge Innovation Project of Chinese Academy of Sciences.

- 
- \* Electronic address: nlwang@aphy.iphy.ac.cn
- <sup>1</sup> S. Nagata, T. Hagino, Y. Seki, and T. Bitoh, *Physics B* **194-196**, 1077 (1994).
  - <sup>2</sup> T. Furubayashi, T. Matsumoto, T. Hagino, and S. Nagata, *J. Phys. Soc. Jpn.* **63**, 3333 (1994).
  - <sup>3</sup> T. Oda, M. Shirai, N. Suzuki, and K. Motizuki, *J. Phys.: Condens. Matter* **7**, 4433 (1995).
  - <sup>4</sup> J. Matsuno, T. Mizokawa, A. Fujimori, D. A. Zatsopin, V. R. Galakhov, E. Z. Kurmaev, Y. Kato and S. Nagata, *Phys. Rev. B* **55**, R15979 (1997).
  - <sup>5</sup> S. Nagata, N. Matsumoto, Y. Kato, T. Furubayashi, T. Matsumoto, J. P. Sanchez and P. Vulliet, *Phys. Rev. B* **58**, 6844 (1998).
  - <sup>6</sup> N. Matsumoto, R. Endoh, S. Nagata, T. Furubayashi and T. Matsumoto *Phys. Rev. B* **60**, 5258 (1999).
  - <sup>7</sup> H. Suzuki, T. Furubayashi, G. Cao, H. Kitazawa, A. Kamimura, K. Hirata, and T. Matsumoto, *J. Phys. Soc. Jpn.* **68**, 2495 (1999).
  - <sup>8</sup> A. T. Burkov, T. Nakama, M. Hedo, K. Shintani, K. Yagasaki, N. Matsumoto, and S. Nagata, *Phys. Rev. B* **61**, 10049 (2000).
  - <sup>9</sup> M. Hayashi, M. Nakayama, T. Nanba, T. Matsumoto, J. Tang, and S. Nagata, *Physica B* **281-282**, 631 (2000).
  - <sup>10</sup> G. Cao, T. Furubayashi, H. Suzuki, H. Kitazawa, T. Matsumoto, Y. Uwatoko, *Phys. Rev. B* **64**, 214514 (2001).
  - <sup>11</sup> P. G. Radaelli, Y. Horibe, M. J. Gutmann, H. Ishibashi, C. H. Chen, R. M. Ibberson, Y. Koyama, Y.-S. Hor, V. Kiryukhin, and S.-W. Cheong, *Nature (London)* **416**, 155 (2001).
  - <sup>12</sup> H. Ishibashi, T. Y. Koo, Y. S. Hor, A. Borissov, P. G. Radaelli, Y. Horibe, S.-W. Cheong, and V. Kiryukhin, *Phys. Rev. B* **66**, 144424 (2002).
  - <sup>13</sup> T. Furubayashi, H. Suzuki, T. Matsumoto, and S. Nagata, *Solid State Communications* **126**, 617 (2003).
  - <sup>14</sup> G. Cao, T. Naka, H. Kitazawa, M. Isobe, and T. Matsumoto, *Phys. Lett. A* **307**, 166 (2003).
  - <sup>15</sup> M. Croft, W. Caliebe, H. Woo, T. A. Tyson, D. Sills, Y. S. Hor, S.-W. Cheong, V. Kiryukhin, and S. J. Oh, *Phys. Rev. B* **67**, 201102(R) (2003).
  - <sup>16</sup> E. J. W. Verwey, *Nature (London)* **144**, 327 (1939); E. J. W. Verwey and P. W. Haayman, *Physica* **8**, 979 (1941).
  - <sup>17</sup> Dipute about the exact ordering in  $\text{Fe}_3\text{O}_4$  still exists. See, for example, a review article: M. Imada, A. Fujimori, and Y. Tokura, *Rev. Mod. Phys.* **70**, 1039 (1988), and a recent work: H. Seo, M. Ogata, and H. Fukuyama, *Phys. Rev. B* **65**, 085107 (2002).
  - <sup>18</sup> N. Matsumoto and S. Nagata, *J. Cryst. Growth* **210**, 772 (2000).
  - <sup>19</sup> C. C. Homes, M. Reedyk, D. A. Crandles, and T. Timusk, *Appl. Opt.* **32**, 2973 (1993).
  - <sup>20</sup> Actually the splitting increases as the transitional metals change from 3d to 5d. This was indicated in the band structure calculations, see ref.<sup>3</sup>
  - <sup>21</sup> J. R. Cullen and E. R. Callen, *Phys. Rev. B* **7**, 397 (1973).